

Anisotropic Dynamical Planckian Scaling of the Quasi-Kagome Kondo Lattice CeRhSn with Strong Valence Fluctuation

Shin-ichi Kimura,^{1,2,3,*} Muhammad Frassetia Lubis,²
Hiroshi Watanabe,^{1,2} Yasuyuki Shimura,⁴ and Toshiro Takabatake⁴

¹*Graduate School of Frontier Biosciences, Osaka University, Suita, Osaka 565-0871, Japan*

²*Department of Physics, Graduate School of Science,
Osaka University, Toyonaka, Osaka 560-0043, Japan*

³*Institute for Molecular Science, Okazaki, Aichi 444-8585, Japan*

⁴*Department of Quantum Matter, AdSE, Hiroshima University, Higashi-Hiroshima, Hiroshima, 739-8530, Japan*
(Dated: February 29, 2024)

The anisotropic electronic structure and Drude response of the quasi-kagome Kondo lattice CeRhSn have been investigated using polarized optical conductivity measurements and first-principles density-functional-theory calculations. Along the hexagonal a - and c -axes, the peaks in the middle-infrared region originating from the hybridization between conduction bands and Ce $4f$ states appear even at room temperature, indicating strong valence fluctuation. Renormalized Drude structures observed at the photon energy below 100 meV, on the other hand, obey the dynamical Planckian scaling below 80 K for $E \parallel a$ and below 200 K for $E \parallel c$, suggesting the non-Fermi liquid behavior due to the quantum criticality. These results indicate that the coexistence of the valence fluctuation and quantum criticality is a consequence of anisotropic magnetic fluctuations based on the Ce quasi-kagome lattice structure.

Characteristic physical properties such as non-BCS superconductivity and giant magnetoresistance emerge near the quantum critical point (QCP) of strongly correlated electron systems [1]. These properties originate from the many-body effect of localized and conduction electron spins, of which heavy-fermion systems and copper-oxide high- T_c superconductors are typical examples. In both materials, strongly correlated quasiparticles appear on the itinerant side of the QCP, and Landau's Fermi-liquid theory explains their behavior [2]. On the other hand, on the localized side of the QCP, magnetism appears due to exchange interactions between localized spins. At this boundary, near the QCP, spin fluctuations dominate, and various properties originating from the strong correlation emerge.

Such strong electron correlation can be regarded as quantum entanglement. Recent theoretical works have been developed at the cross-points of condensed matter, elementary-particle physics, and quantum-information theory [3, 4]. These developments claim that simple principles, namely Planckian dissipation, may surprisingly govern the physics of such matter, where the relaxation time of quasiparticles of strongly correlated electron systems is determined as the Planckian time $\hbar/k_B T$ [5]. This phenomenon mainly manifests in fundamental physical properties, such as a linear increase in electrical resistivity with temperature [4, 6, 7]. It is also expected to appear in many physical quantities, for instance, its relationship to self-energies observed in photoelectron spectra and the Drude response in optical conductivity [$\sigma_1(\omega)$] spectra [5]. The Drude response is discussed to scale (Dynamical Planckian Scaling: DPS) with the photon energy normalized by temperature ($\hbar\omega/k_B T$) [8, 9], and has been reported in high- T_c cuprates [10, 11] and

a heavy-fermion material YbRh₂Si₂ [12]. However, it is currently debated whether quasiparticles in heavy-fermion systems are Planckian or not [13].

One of those predicted to follow the DPS is CeRhSn [14]. CeRhSn is a valence-fluctuation material [15, 16] with a hexagonal ZrNiAl-type crystal structure (No. 189, $P62m$) [17], as shown in the inset of Fig. 1. The Ce atoms assemble a quasi-kagome lattice in the ab -plane. The electrical resistivity has a large anisotropy, *i.e.*, the electrical resistivity along the a -axis is about 3–5 times higher than that along the c -axis, in contrast to the low resistivity ratio of 1.4 at most in LaRhSn without $4f$ electrons [18]. The large anisotropy in CeRhSn originates from anisotropic magnetic interactions, and the material is located near the antiferromagnetic instability [19]. Non-Fermi-liquid (NFL) behavior appears below 1 K in the specific heat and thermal expansion, originating from this geometric frustration in the quasi-kagome structure of the Ce ions [20]. The anisotropic spin fluctuations are also essential for the NFL behavior [21]. Investigating how the anisotropic geometrical frustration affects the electronic structure and whether the Drude response follows the DPS in CeRhSn is worthwhile.

In this Letter, we report the significantly different Drude response of the polarized $\sigma_1(\omega)$ spectra of CeRhSn along the a - and c -axes and discuss the interplay between the valence fluctuation behavior due to the c - f hybridization and the NFL character of the quasiparticles. $\sigma_1(\omega)$ spectra are sensitive to the c - f hybridization and the heavy quasiparticles' behaviors [22–24]. The polarized $\sigma_1(\omega)$ spectra of CeRhSn present strong anisotropies in the electronic structure and the Drude response along the a - and c -axes. Along both axes, a $4f$ spin-orbit doublet showing c - f hybridization formation appears at photon

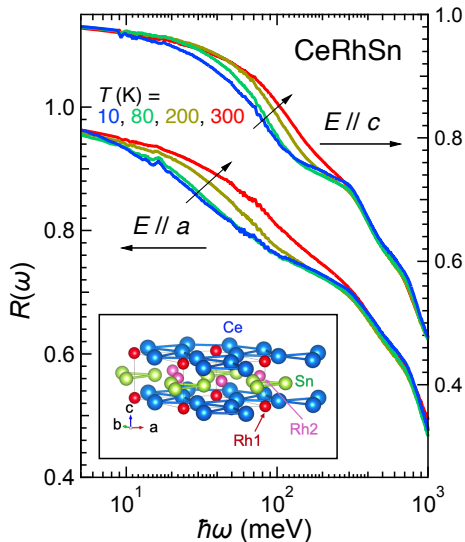


FIG. 1. Temperature-dependent polarized reflectivity [$R(\omega)$] spectra of CeRhSn in the photon energy $\hbar\omega$ range of 5 – 1000 meV. A fine structure for $E \parallel a$ at $\hbar\omega \sim 15$ meV originates from phonons (not discussed here). (Inset) Crystal structure of CeRhSn with a quasi-kagome Ce lattice in the basal plane. Rh atoms have two different sites, namely Rh1 and Rh2, corresponding to the different densities of states shown in Fig. 3.

energies ($\hbar\omega$) of about 300 and 600 meV, even at room temperature, indicating strong valence fluctuation. On the other hand, a Drude response below 100 meV reflects the formation of heavy quasiparticles. As the temperature decreases, the Drude weight moves to the low-energy side in both axes, suggesting a renormalization of heavy quasiparticles. Analysis of the Drude structure reveals that the DPS holds below 80 K for $E \parallel a$ and below 200 K for $E \parallel c$, and low-temperature DPS behaviors suggest the NFL along both axes. These results imply that the magnetic fluctuation strongly couples to charge carriers via the c - f hybridization and induces NFL behavior.

Single crystals of CeRhSn were grown by the Czochralski method in a radio-frequency induction furnace [18]. The samples were polished to mirror surfaces with 3MTM Lapping Film Sheets (0.3 Micron Grade) along the crystal axes to measure near-normal-incident polarized optical reflectivity [$R(\omega)$] spectra. The $R(\omega)$ spectra were acquired in a wide $\hbar\omega$ range of 5 meV – 30 eV to ensure accurate Kramers-Kronig analysis (KKA) [25]. Infrared and terahertz measurements at $\hbar\omega = 5$ –30 meV and 0.01–1.5 eV have been performed using $R(\omega)$ measurement setups with Martin-Puplett and Michelson FTIR spectrometers, respectively, combined with several light sources, beam splitters, detectors, and polarizers. Measurements were performed using the system that automatically de-

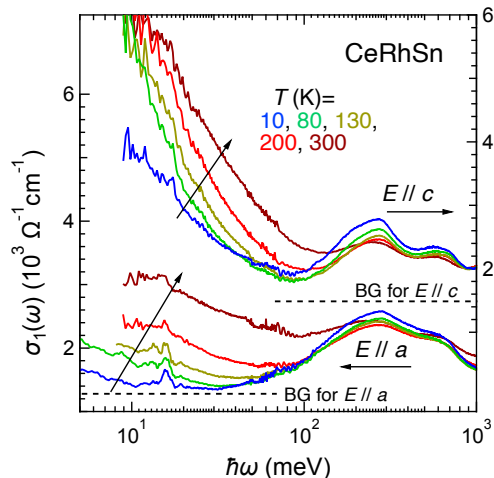


FIG. 2. Temperature-dependent optical conductivity [$\sigma_1(\omega)$] spectra of CeRhSn with $E \parallel a$ (bottom) and $E \parallel c$ (top). The peaks at $\hbar\omega \sim 15$ meV in both axes originate from phonons. BG lines for both axes are the expected background spectra [$\sigma_{BG}(\omega)$] due to the weak interacting carriers for the DPS analysis in Fig. 4.

termines the sample position at varying temperatures of 6–300 K [26]. The absolute values of $R(\omega)$ spectra were determined with the *in-situ* gold evaporation method. Obtained polarized $R(\omega)$ spectra of CeRhSn are shown in Fig. 1. In the $\hbar\omega$ range of 1.5–30 eV, the $R(\omega)$ spectrum was acquired only at 300 K by using the synchrotron radiation setup at the beamline 3B [27] of UVSOR-III Synchrotron [28], and connected to the spectra for $\hbar\omega \leq 1.5$ eV for conducting KKA. In order to obtain $\sigma_1(\omega)$ via KKA of $R(\omega)$, the spectra were extrapolated below 5 meV with a Hagen-Rubens function [$R(\omega) = 1 - \{2\omega/(\pi\sigma_{DC})\}^{1/2}$] due to the metallic $R(\omega)$ spectra, and above 30 eV with a free-electron approximation $R(\omega) \propto \omega^{-4}$ [29]. Here, the direct current conductivity (σ_{DC}) values were adopted from the experimental values [18]. The extrapolations were confirmed not to severely affect the $\sigma_1(\omega)$ spectra at $\hbar\omega \sim 5$ – 100 meV, which is the main part of this paper.

First-principles density-functional-theory (DFT) calculations of the band structure have been performed by using the WIEN2K code, including spin-orbit interaction [30], to explain the experimental $\sigma_1(\omega)$ spectra. We used lattice parameters reported in Ref. [18] for the calculations. The calculated band structure (shown in Fig. 3(a)) is consistent with the previous reports [15, 31, 32].

The temperature dependence of the $\sigma_1(\omega)$ spectra of CeRhSn along the a - and c -axes is shown in Fig. 2. The significant axial dependence of the spectra reflects the anisotropy of the electronic state. The $4f$ spin-orbit doublet along both axes at $\hbar\omega \sim 300$ and 600 meV, namely

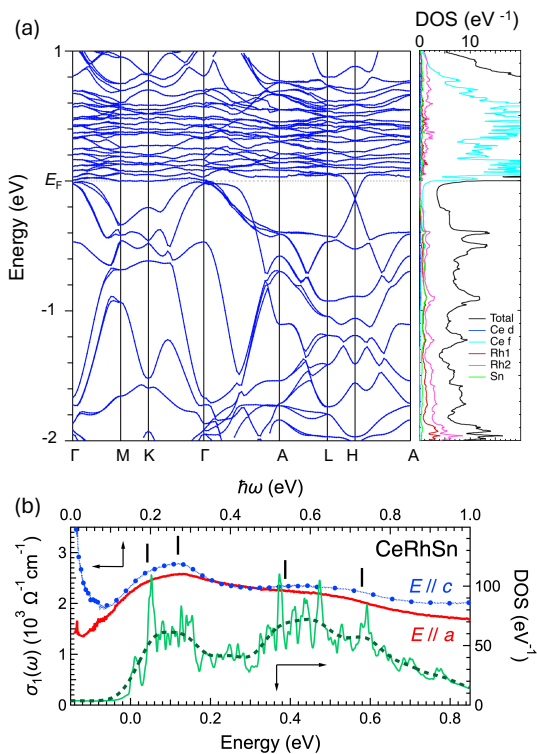


FIG. 3. (a) Band structure and density of states (DOS) of CeRhSn by the DFT calculation with spin-orbit interaction. (b) Anisotropic optical conductivity $[\sigma_1(\omega)]$ spectra of the mid-IR peaks of CeRhSn at $T = 10$ K compared with the unoccupied DOS (thin solid line). The energy of the DOS is shifted by 0.15 eV from the $\hbar\omega$ of $\sigma_1(\omega)$ spectra. The dashed line is the smoothed curve of the DOS. Vertical lines of $\sigma_1(\omega)$ spectra indicate the structures corresponding to those in the DOS.

mid-IR peaks, originating from the strong c - f hybridization [22], appears in both directions, even at 300 K. On the other hand, a clear anisotropic Drude response appears at $\hbar\omega \leq 100$ meV, which is consistent with the anisotropic electrical resistivity [18]. As the nonmagnetic counterpart LaRhSn has a weak anisotropy in the electrical resistivity, the axial dependence of this Drude structure is attributed to the anisotropic magnetic interactions.

Firstly, the mid-IR peaks are compared to the band structure calculations. Figure 3(a) shows the band structure and the density of states (DOS) of CeRhSn by the DFT calculations. The high DOS above the 0 eV (= Fermi energy; E_F) originates from the Ce 4*f* unoccupied states. The calculated band structure is regarded as fully itinerant; therefore, comparing the experimental $\sigma_1(\omega)$ spectra to the band calculation helps check the itinerant character [23]. In Fig. 3(b), the mid-IR peaks at about 0.3 and 0.6 eV obtained at $T = 10$ K are compared to the unoccupied DOS, shown at the bottom. The DOS curve was smoothed to the dashed line to compare to the

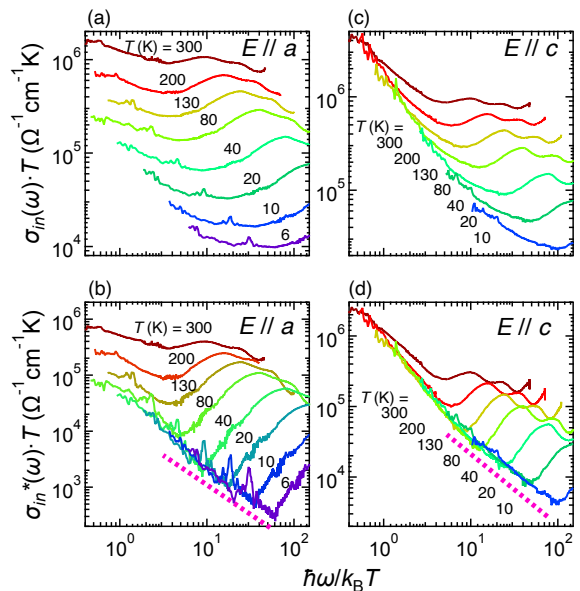


FIG. 4. Dynamical Planckian scaling plot as a function of $\hbar\omega/k_B T$ as shown in Eq. 1 for $E \parallel a$ (a, b) and $E \parallel c$ (c, d). In (a) and (c), the intrinsic optical conductivity $[\sigma_{in}(\omega)]$ spectra are only used, but in (b) and (d), the constant backgrounds originating from carriers with weak electron correlation (BG lines in Fig. 2) are subtracted. The dotted lines in (b) and (d) indicate constants of $\sigma_{in}^*(\omega) \cdot \hbar\omega/k_B$.

$\sigma_1(\omega)$ spectra. Notably, the smoothed DOS resembles the shape of the mid-IR peaks of the $\sigma_1(\omega)$ spectrum. Therefore, in addition to the appearance of the mid-IR peaks at 300 K, the good correspondence of the mid-IR peaks to the DOS confirms the strong c - f hybridization strength [22, 33], which is consistent with previous photoelectron works [34, 35]. It should be noted that the 0 eV of the DOS is aligned with the 0.15 eV of the $\sigma_1(\omega)$ spectrum for better correspondence, indicating that the initial state of photo-excitation is 0.15 eV below the E_F . As expected, the DOS curve in Fig. 3(a) shows a step-like structure in the valence band at about -0.15 eV.

Next, we discuss whether the temperature dependence of the Drude component can be explained with DPS. In Refs. [9] and [12], it is shown that if DPS is realized, the temperature dependence of the $\sigma_1(\omega)$ spectrum has a relationship;

$$\sigma_{in}(\omega) \cdot T = f(\hbar\omega/k_B T), \quad (1)$$

where $\sigma_{in}(\omega)$ is the real-part intrinsic optical conductivity. The observed $\sigma_1(\omega)$ spectrum and the zero-temperature residual optical conductivity σ_{res} (= inverse residual resistivity) have the following relation;

$$\sigma_1(\omega)^{-1} = \sigma_{in}(\omega)^{-1} + \sigma_{res}^{-1}. \quad (2)$$

σ_{res} is about $7800 \Omega^{-1}\text{cm}^{-1}$ in $E \parallel a$ and about $10000 \Omega^{-1}\text{cm}^{-1}$ in $E \parallel c$ [18]. The calculated $\sigma_{in}(\omega) \cdot T$

spectra are shown in Figs. 4(a, c). At a glance at these figures, the Drude response in both directions does not seem to follow the DPS.

However, the $\sigma_{in}(\omega)$ spectra comprise the contributions of “heavy” and “light” quasiparticles with and without strong electron correlation, respectively. The individual contributions from heavy and light quasiparticles manifest in the several effective masses appearing in quantum oscillations [36]. In $\sigma_1(\omega)$ spectra, the evidence of the light quasiparticles appears as a background of the Drude structure [37, 38]. Then, we derive the heavy quasiparticles’ intrinsic optical conductivity $\sigma_{in}^*(\omega)$ spectra from the $\sigma_{in}(\omega)$ spectra by subtracting the light quasiparticles’ background $\sigma_{BG}(\omega)$;

$$\sigma_{in}^*(\omega) = \sigma_{in}(\omega) - \sigma_{BG}(\omega). \quad (3)$$

Here, we assumed constant $\sigma_{BG}(\omega)$ as $1300 \Omega^{-1}\text{cm}^{-1}$ for $E \parallel a$ and $1500 \Omega^{-1}\text{cm}^{-1}$ for $E \parallel c$ as shown by the BG lines in Fig. 2. The DPS plot of $\sigma_{in}^*(\omega)$ is shown in Figs. 4(b, d). These figures pronounce that the DPS is realized at temperatures below 80 K for $E \parallel a$ and below 200 K for $E \parallel c$. Therefore, it could be concluded that the Drude responses along both axes follow the DPS by subtracting $\sigma_{BG}(\omega)$ from $\sigma_{in}(\omega)$.

The maximum magnetic electrical resistivity along the a -axis appears at about 80 K, below which the coherent Kondo lattice is realized [18]. The evidence suggests that the DPS for $E \parallel a$ appears in the coherence state. On the other hand, with decreasing temperature, the electrical resistivity along the c -axis monotonically decreases with a slight shoulder structure at $T \sim 50$ K, suggesting a weak Kondo lattice formation. Therefore, the DPS behavior for $E \parallel c$ at a relatively high temperature of about 200 K may originate from another reason, such as an electron-phonon coupling as discussed for the $\sigma_1(\omega)$ of doped silicon [39].

In the low-temperature regions where the DPS holds in Figs. 4(b, d), $\sigma_{in}^*(\omega) \cdot T$ is inversely proportional to $\hbar\omega/k_B T$. This relationship indicates that $\sigma_{in}^*(\omega) \cdot \hbar\omega/k_B$ is constant, as shown by dotted lines. The constant values of $\sigma_{in}^*(\omega) \cdot \hbar\omega/k_B$ can be evaluated as about $2 \times 10^4 \Omega^{-1}\text{cm}^{-1}\text{K}$ for $E \parallel a$ and $3 \times 10^5 \Omega^{-1}\text{cm}^{-1}\text{K}$ for $E \parallel c$, indicating a large anisotropy in the $\sigma_{in}^*(\omega) \cdot \hbar\omega/k_B$ values. CeRhSn exhibits an NFL behavior in the specific heat and thermal expansion down to 60 mK [20]. Still, the spin fluctuations are rapidly suppressed by a magnetic field applied along the c -axis rather than the a -axis [21]. Therefore, the anisotropic $\sigma_{in}^*(\omega) \cdot \hbar\omega/k_B$ values can be explained by the anisotropic NFL behavior.

It should be noted that Prochaska *et al.* presented that YbRh₂Si₂ also has the constant $\sigma_{in}(\omega) \cdot \hbar\omega/k_B$ of about $3 \cdot 10^5 \Omega^{-1}\text{cm}^{-1}\text{K}$ for $T \leq 15$ K [12]. This value coincides with that for $E \parallel c$ of CeRhSn, so the NFL behavior in this direction may be similar to YbRh₂Si₂. The value $\sigma_{in}(\omega) \cdot \hbar\omega/k_B$ value for $E \parallel a$ is one order of magnitude smaller than that for $E \parallel c$. Since the DPS appears only

in the coherent Kondo lattice state for $E \parallel a$, it would be due to the geometrical frustration of the quasi-kagome structure. These results imply that the heavy fermion systems of CeRhSn and YbRh₂Si₂ follow the same DPS function, $\sigma_{in}(\omega) \cdot \hbar\omega/k_B = \text{constant}$, but have individual values, which may provide a meaningful result. Further data should be added to establish a universal DPS in heavy-fermion systems.

In most three-dimensional Ce-based heavy-fermion materials in the vicinity of QCP, the mid-IR peaks are slightly visible owing to the relatively weak c - f hybridization intensity [22, 40–42]. However, the mid-IR peaks clearly appear in CeRhSn, being the hallmark of strong valence fluctuation. The simultaneous appearance of the valence fluctuation and DPS owing to the quasi-kagome structure describes that the quantum criticality of CeRhSn is different from usual NFL heavy-fermions like CeCu_{6-x}Au_x, where AFM correlations are responsible for the quantum criticality [43].

In conclusion, polarized optical conductivity measurements and first-principles DFT calculations have investigated the anisotropic electronic structure and Drude response of the quasi-kagome Kondo lattice material CeRhSn. Along the hexagonal a - and c -axes, the $4f$ spin-orbit doublet showing the strong c - f hybridization appears even at room temperature, indicating the strong valence fluctuation behavior. On the other hand, a renormalized Drude response at $\hbar\omega \leq 100$ meV indicates the formation of heavy quasiparticles. Analysis of the Drude structure shows that it follows the DPS along both axes but has different constant $\sigma_{in}^*(\omega) \cdot \hbar\omega/k_B$ values, resulting from the anisotropic magnetic fluctuations based on the Ce quasi-kagome lattice. These findings support that the quantum criticality of CeRhSn coexists with the valence fluctuation. This work should motivate further investigation to clarify whether the anisotropic DPS commonly describes low-temperature responses of low-dimensional NFL heavy-fermion materials.

We thank UVSOR Synchrotron staff members for their support during synchrotron radiation experiments. Part of this work was performed under the Use-of-UVSOR Synchrotron Facility Program (Proposals No. 23IMS6016) of the Institute for Molecular Science, National Institutes of Natural Sciences. This work was partly supported by JSPS KAKENHI (Grant Nos. 23H00090, 17K05545).

* kimura.shin-ichi.fbs@osaka-u.ac.jp

- [1] S. Sachdev, Quantum Phase Transitions (Cambridge University Press, 2011).
- [2] L. D. Landau, Soviet Physics JETP **35**, 70 (1959).
- [3] S. A. Hartnoll, J. Polchinski, E. Silverstein, and D. Tong, J. High Energy Phys. **2010**, 120 (2010).
- [4] J. Zaanen, SciPost Phys. **6**, 061 (2019).

- [5] S. A. Hartnoll and A. P. Mackenzie, *Rev. Mod. Phys.* **94**, 041002 (2022).
- [6] J. A. N. Bruin, H. Sakai, R. S. Perry, and A. P. Mackenzie, *Science* **339**, 804 (2013).
- [7] G. Grissonnanche, Y. Fang, A. Legros, S. Verret, F. Laliberté, C. Collignon, J. Zhou, D. Graf, P. A. Goddard, L. Taillefer, and B. J. Ramshaw, *Nature* **595**, 667 (2021).
- [8] G. T. Horowitz, J. E. Santos, and D. Tong, *J. High Energy Phys.* **2012**, 168 (2012).
- [9] X. Li, J. Kono, Q. Si, and S. Paschen, *Frontiers in Electronic Materials* **2**, 934691 (2023).
- [10] D. van der Marel, H. J. A. Molegraaf, J. Zaanen, Z. Nussinov, F. Carbone, A. Damascelli, H. Eisaki, M. Greven, P. H. Kes, and M. Li, *Nature* **425**, 271 (2003).
- [11] B. Michon, C. Berthod, C. W. Rischau, A. Ataei, L. Chen, S. Komiya, S. Ono, L. Taillefer, D. van der Marel, and A. Georges, *Nat. Commun.* **14**, 3033 (2023).
- [12] L. Prochaska, X. Li, D. C. MacFarland, A. M. Andrews, M. Bonta, E. F. Bianco, S. Yazdi, W. Schrenk, H. Detz, A. Limbeck, Q. Si, E. Ringe, G. Strasser, J. Kono, and S. Paschen, *Science* **367**, 285 (2020).
- [13] M. Taupin and S. Paschen, *Crystals (Basel)* **12**, 251 (2022).
- [14] A. Kandala, H. Hu, Q. Si, and K. Ingersent, (2022), arXiv:2206.01174 [cond-mat.str-el].
- [15] M. Gamża, A. Ślebarski, and H. Rosner, *Eur. Phys. J. B* **67**, 483 (2009).
- [16] O. Niehaus, P. M. Abdala, and R. Pöttgen, *Zeitschrift für Naturforschung B* **70**, 253 (2015).
- [17] R. Pöttgen and B. Chevalier, *Zeitschrift für Naturforschung B* **70**, 289 (2015).
- [18] M. S. Kim, Y. Echizen, K. Umeo, S. Kobayashi, M. Sera, P. S. Salamakha, O. L. Sologub, T. Takabatake, X. Chen, T. Tayama, T. Sakakibara, M. H. Jung, and M. B. Maple, *Phys. Rev. B: Condens. Matter Mater. Phys.* **68**, 054416 (2003).
- [19] H. Tou, M. S. Kim, T. Takabatake, and M. Sera, *Phys. Rev. B Condens. Matter* **70**, 100407 (2004).
- [20] Y. Tokiwa, C. Stingl, M.-S. Kim, T. Takabatake, and P. Gegenwart, *Sci. Adv.* **1**, e1500001 (2015).
- [21] S. Kittaka, Y. Kono, S. Tsuda, T. Takabatake, and T. Sakakibara, *J. Phys. Soc. Jpn.* **90**, 064703 (2021).
- [22] S.-I. Kimura, Y. S. Kwon, Y. Matsumoto, H. Aoki, and O. Sakai, *J. Phys. Soc. Jpn.* **85**, 083702 (2016).
- [23] S.-I. Kimura, Y. S. Kwon, C. Krellner, and J. Sichelschmidt, *Electronic Structure* **3**, 024007 (2021).
- [24] S. Kirchner, S. Paschen, Q. Chen, S. Wirth, D. Feng, J. D. Thompson, and Q. Si, *Rev. Mod. Phys.* **92**, 011002 (2020).
- [25] S.-I. Kimura and H. Okamura, *J. Phys. Soc. Jpn.* **82**, 021004 (2013).
- [26] S.-I. Kimura, *Jasco Report* **50**, 6 (2008).
- [27] K. Fukui, R.-I. Ikematsu, Y. Imoto, M. Kitaura, K. Nakagawa, T. Ejima, E. Nakamura, M. Sakai, M. Hasumoto, and S.-I. Kimura, *J. Synchrotron Radiat.* **21**, 452 (2014).
- [28] H. Ota, E. Salehi, M. Fujimoto, K. Hayashi, T. Horigome, H. Iwayama, M. Katoh, N. Kondo, S. Makita, F. Matsui, H. Matsuda, T. Mizukawa, A. Minakuchi, E. Nakamura, M. Nagasaka, Y. Okano, T. Ohigashi, M. Sakai, K. Sugita, K. Tanaka, Y. Taira, F. Teshima, J.-I. Yamazaki, T. Yano, H. Yuzawa, and S. Kera, *J. Phys. Conf. Ser.* **2380**, 012003 (2022).
- [29] M. Dressel and G. Grüner, *Electrodynamics of Solids* (Cambridge University Press, 2002).
- [30] P. Blaha, K. Schwarz, F. Tran, R. Laskowski, G. K. H. Madsen, and L. D. Marks, *J. Chem. Phys.* **152**, 074101 (2020).
- [31] A. Ślebarski, T. Zawada, J. Spalek, and A. Jezierski, *Phys. Rev. B Condens. Matter* **70**, 235112 (2004).
- [32] A. F. Al Alam, S. F. Matar, N. Ouaini, and M. Nakhil, *Eur. Phys. J. B* **65**, 491 (2008).
- [33] H. Okamura, T. Watanabe, M. Matsunami, T. Nishihara, N. Tsujii, T. Ebihara, H. Sugawara, H. Sato, Y. Onuki, Y. Isikawa, T. Takabatake, and T. Nanba, *J. Phys. Soc. Jpn.* **76**, 023703 (2007).
- [34] K. Shimada, H. Namatame, M. Taniguchi, M. Higashiguchi, S.-I. Fujimori, Y. Saitoh, A. Fujimori, M. S. Kim, D. Hirata, and T. Takabatake, *Physica B Condens. Matter* **378-380**, 791 (2006).
- [35] M. Sundermann, A. Marino, A. Gloskovskii, C. Yang, Y. Shimura, T. Takabatake, and A. Severing, *Phys. Rev. B: Condens. Matter Mater. Phys.* **104**, 235150 (2021).
- [36] Y. Ōnuki, R. Settai, K. Sugiyama, T. Takeuchi, T. C. Kobayashi, Y. Haga, and E. Yamamoto, *J. Phys. Soc. Jpn.* **73**, 769 (2004).
- [37] A. M. Awasthi, L. Degiorgi, G. Grüner, Y. Dalichaouch, and M. B. Maple, *Phys. Rev. B Condens. Matter* **48**, 10692 (1993).
- [38] L. Degiorgi, *Rev. Mod. Phys.* **71**, 687 (1999).
- [39] M. van Exter and D. Grischkowsky, *Phys. Rev. B Condens. Matter* **41**, 12140 (1990).
- [40] F. Marabelli and P. Wachter, *Phys. Rev. B Condens. Matter* **42**, 3307 (1990).
- [41] E. J. Singley, D. N. Basov, E. D. Bauer, and M. B. Maple, *Phys. Rev. B: Condens. Matter Mater. Phys.* **65**, 161101 (2002).
- [42] S.-I. Kimura, T. Iizuka, and Y.-S. Kwon, *J. Phys. Soc. Jpn.* **78**, 013710 (2009).
- [43] H. v. Löhneysen, A. Rosch, M. Vojta, and P. Wölfle, *Rev. Mod. Phys.* **79**, 1015 (2007).